J|A|C|S
ARTICLES
Published on Web 10/17/2006

A Mechanistic Dichotomy in Scandium Ion-Promoted Hydride Transfer of an NADH Analogue: Delicate Balance between One-Step Hydride-Transfer and Electron-Transfer Pathways

Junpei Yuasa, Shunsuke Yamada, and Shunichi Fukuzumi*

Contribution from the Department of Material and Life Science, Division of Advanced Science and Biotechnology, Graduate School of Engineering, Osaka University, SORST, Japan Science and Technology Agency (JST), Suita, Osaka 565-0871, Japan

Received July 6, 2006; E-mail: fukuzumi@chem.eng.osaka-u.ac.jp

Abstract: The rate constant (k_H) of hydride transfer from an NADH analogue, 9,10-dihydro-10-methylacridine ($AcrH_2$), to 1-(*p*-tolylsulfinyl)-2,5-benzoquinone (TolSQ) increases with increasing Sc^{3+} concentration ([Sc^{3+}]) to reach a constant value, when all TolSQ molecules form the TolSQ−Sc^{3+} complex. When $AcrH_2$ is replaced by the dideuterated compound ($AcrD_2$), however, the rate constant (k_D) increases linearly with an increase in [Sc^{3+}] without exhibiting a saturation behavior. In such a case, the primary kinetic deuterium isotope effect (k_H/k_D) decreases with increasing [Sc^{3+}]. On the other hand, the rate constant of Sc^{3+}-promoted electron transfer from tris(2-phenylpyridine)iridium [$Ir(ppy)_3$] to TolSQ also increases linearly with increasing [Sc^{3+}] at high concentrations of Sc^{3+} due to formation of a 1:2 complex between $TolSQ^{\bullet-}$ and Sc^{3+}, [$TolSQ^{\bullet-}$−(Sc^{3+})$_2$], which was detected by ESR. The significant difference with regard to dependence of the rate constant of hydride transfer on [Sc^{3+}] between $AcrH_2$ and $AcrD_2$ in comparison with that of Sc^{3+}-promoted electron transfer indicates that the reaction pathway is changed from one-step hydride transfer from $AcrH_2$ to the TolSQ−Sc^{3+} complex to Sc^{3+}-promoted electron transfer from $AcrD_2$ to the TolSQ−Sc^{3+} complex, followed by proton and electron transfer. Such a change between two reaction pathways, which are employed simultaneously, is also observed by simple changes of temperature and concentration of Sc^{3+}.

Introduction

Dihydronicotinamide adenine dinucleotide (NADH) acts as an important source of two electrons and a proton (equivalent to a hydride ion) in biological redox systems.[1] There is a mechanistic dichotomy whether hydride transfer from NADH and analogues to a hydride acceptor (A) occurs via one-step hydride transfer (H^-) or electron transfer followed by proton−electron transfer ($e^- + H^+ + e^-$) as shown in Scheme 1.[2−6] The mechanistic borderline between one-step and multistep reactions has always been of large general interest to chemists. Do the mechanisms merge at the borderline; i.e., is there a mechanistic continuity. Or are both pathways employed simultaneously? Mechanisms of hydride-transfer reactions of NADH analogues have so far been extensively studied in the reactions with various inorganic[7−12] and organic[13−24] substrates including the effect of metal ions.[25−31] However, there has been a long standing ambiguity as to the mechanistic borderline in the hydride-transfer reactions of NADH and analogues (Scheme 1).[2−6]

(1) Stryer, L. *Biochemistry*, 3rd ed; Freeman: New York, 1988; Chapter 17.
(2) Gebicki, J.; Marcinek, A.; Zielonka, J. *Acc. Chem. Res.* **2004**, *37*, 379.
(3) (a) Fukuzumi, S. In *Advances in Electron-Transfer Chemistry*; Mariano, P. S., Ed.; JAI Press: Greenwich, CT, 1992; pp 67−175. (b) Fukuzumi, S.; Tanaka, T. In *Photoinduced Electron Transfer*; Fox, M. A., Chanon, M., Eds.; Elsevier: Amsterdam, 1988; Part C, Chapter 10.
(4) (a) Eisner, U.; Kuthan, J. *Chem. Rev.* **1972**, *72*, 1. (b) Stout, D. M.; Meyers, A. I. *Chem. Rev.* **1982**, *82*, 223.
(5) Fukuzumi, S.; Itoh, S. *Antioxid. Redox Signaling* **2001**, *3*, 807.
(6) (a) Zhu, X.-Q.; Yang, Y.; Zhang, M.; Cheng, J.-P. *J. Am. Chem. Soc.* **2003**, *125*, 15298. (b) Zhu, X.-Q.; Cao, L.; Liu, Y.; Yang, Y.; Lu, J.-Y.; Wang, J.-S.; Cheng, J.-P. *Chem.—Eur. J.* **2003**, *9*, 3937. (c) Zhu, X.-Q.; Li, H.-R.; Li, Q.; Ai, T.; Lu, J.-Y.; Yang, Y.; Cheng, J.-P. *Chem.—Eur. J.* **2003**, *9*, 871. (d) Cheng, J.-P.; Lu, Y.; Zhu, X.; Mu, L. *J. Org. Chem.* **1998**, *63*, 6108. (e) Cheng, J.-P.; Handoo, K. L.; Xue, J.; Parker, V. D. *J. Org. Chem.* **1993**, *58*, 5050.
(7) Carlson, B. W.; Miller, L. L.; Neta, P.; Grodkowski, J. *J. Am. Chem. Soc.* **1984**, *106*, 7233.
(8) (a) Powell, M. F.; Wu, J. C.; Bruice, T. C. *J. Am. Chem. Soc.* **1984**, *106*, 3850. (b) Sinha, A.; Bruice, T. C. *J. Am. Chem. Soc.* **1984**, *106*, 7291.
(9) (a) Matsuo, T.; Mayer, J. M. *Inorg. Chem.* **2005**, *44*, 2150. (b) Larsen, A. S.; Wang, K.; Lockwood, M. A.; Rice, G. L.; Won, T.-J.; Lovell, S.; Sadílek, M.; Turecek, F.; Mayer, J. M. *J. Am. Chem. Soc.* **2002**, *124*, 10112.
(10) (a) Pestovsky, O.; Bakac, A.; Espenson, J. H. *J. Am. Chem. Soc.* **1998**, *120*, 13422. (b) Pestovsky, O.; Bakac, A.; Espenson, J. H. *Inorg. Chem.* **1998**, *37*, 1616.
(11) Afanasyeva, M.; Taraban, M. B.; Purtov, P. A.; Leshina, T. V.; Grissom, C. B. *J. Am. Chem. Soc.* **2006**, *128*, 8651.
(12) Fukuzumi, S.; Kondo, Y.; Tanaka, T. *J. Chem. Soc., Perkin Trans. 2* **1984**, 673.
(13) Lee, I.-S. H.; Jeoung, E. H.; Kreevoy, M. M. *J. Am. Chem. Soc.* **1997**, *119*, 2722.
(14) (a) Powell, M. F.; Bruice, T. C. *J. Am. Chem. Soc.* **1983**, *105*, 1014. (b) Chipman, D. M.; Yaniv, R.; van Eikeren, P. *J. Am. Chem. Soc.* **1980**, *102*, 3244.
(15) (a) Ohno, A.; Yamamoto, H.; Oka, S. *J. Am. Chem. Soc.* **1981**, *103*, 2041. (b) Ohno, A.; Shio, T.; Yamamoto, H.; Oka, S. *J. Am. Chem. Soc.* **1981**, *103*, 2045. (c) Ohno, A.; Ishikawa, Y.; Yamazaki, N.; Okamura, M.; Kawai, Y. *J. Am. Chem. Soc.* **1998**, *120*, 1186.
(16) (a) Tanner, D. D.; Kharrat, A.; Oumar-Mahamat, H. *Can. J. Chem.* **1990**, *68*, 1662. (b) Tanner, D. D.; Kharrat, A. *J. Org. Chem.* **1988**, *53*, 1646. (c) Liu, Y.-C.; Li, B.; Guo, Q.-X. *Tetrahedron* **1995**, *51*, 9671.
(17) (a) Kim, Y.; Truhlar, D. G.; Kreevoy, M. M. *J. Am. Chem. Soc.* **1991**, *113*, 7837. (b) Kotchevar A. T.; Kreevoy, M. M. *J. Phys. Chem.* **1991**, *95*, 10345. (c) Kreevoy M. M.; Kotchevar, A. T. *J. Am. Chem. Soc.* **1990**, *112*, 3579.
(18) (a) Anne, A.; Moiroux, J. *J. Org. Chem.* **1990**, *55*, 4608. (b) Anne, A.; Moiroux, J. *Can. J. Chem.* **1995**, *73*, 531. (c) Anne, A.; Moiroux J.; Savéant, J.-M. *J. Am. Chem. Soc.* **1993**, *115*, 10224.
(19) Ellis, W. W.; Raebiger, J. W.; Curtis, C. J.; Bruno, J. W.; DuBois, D. L. *J. Am. Chem. Soc.* **2004**, *126*, 2738.
(20) Fukuzumi, S.; Nishizawa, N.; Tanaka, T. *J. Org. Chem.* **1984**, *49*, 3571.

10.1021/ja064708a CCC: $33.50

Scheme 1

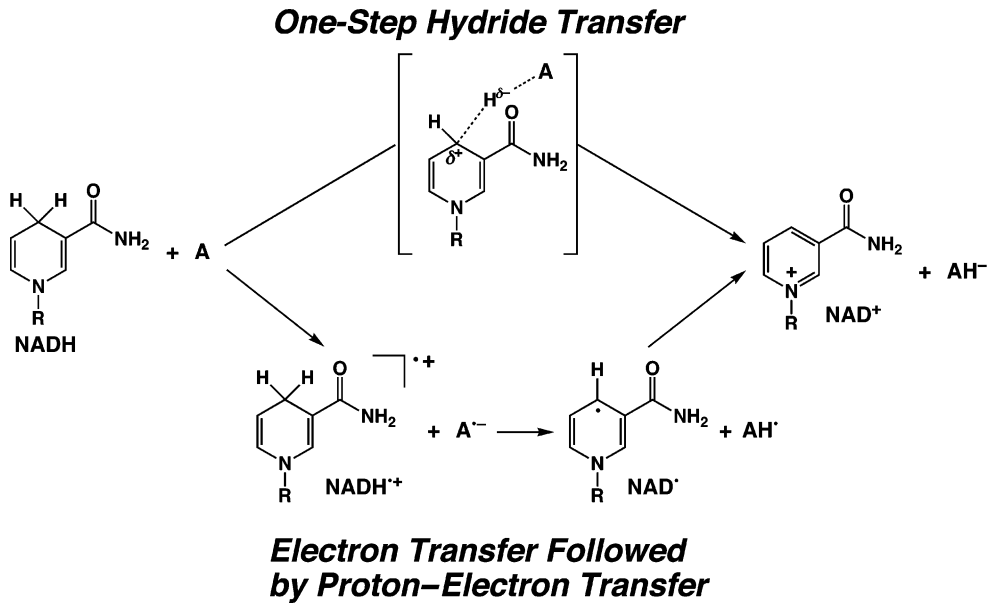

The effects of the metal ion on the mechanistic borderline in the hydride-transfer reactions of NADH and analogues have particularly attracted interest because of the essential role of metal ions in the redox reactions of nicotinamide coenzymes in the native enzymatic system.[3−5,25−31] Metal ions (M^{n+}) acting as a Lewis acid are known to promote hydride-transfer reactions of NADH analogues[25−31] as well as electron transfer from electron donors (D) to electron acceptors, such as *p*-benzoquinones (Q), which have been commonly used in the hydride-transfer and electron-transfer reactions of NADH analogues, where M^{n+} bind to the product radical anion.[32−41] Semiquinone radical anions ($Q^{\bullet-}$) derived from *p*-benzoquinones form not only simple 1:1 complexes ($Q^{\bullet-}-M^{n+}$) with M^{n+} but also more intricate complexes with M^{n+}, i.e., 1:2 complexes [$Q^{\bullet-}-(M^{n+})_2$] as shown in Scheme 2a.[29,32] In such a case, the rate constants of M^{n+}-promoted electron-transfer reactions increase with increasing M^{n+} concentration ([M^{n+}]), exhibiting a second-order dependence on [M^{n+}] at high concentrations due to formation of the 1:2 complexes [$Q^{\bullet-}-(M^{n+})_2$] (Scheme 2a).[29,32] Virtually the same second-order dependence is observed in M^{n+}-promoted hydride-transfer reactions of NADH analogues, such as 1-benzyl-1,4-dihydronicotinamide (BNAH), when the hydride-transfer reactions proceed via an electron-transfer pathway, which is promoted by the formation of 1:2 complexes [$Q^{\bullet-}-(M^{n+})_2$] (Scheme 2b).[29,32] In contrast to the case of an electron-transfer pathway, a one-step hydride-transfer pathway is not promoted by M^{n+}, because M^{n+} has generally no interaction with Q.[29,32]

If a hydride acceptor (A) has a metal ion-binding site, the complex formation of A with M^{n+} ($A-M^{n+}$), which results in enhancement of both electrophilicity and electron-acceptor ability of A, would provide a delicate balance between the two reaction pathways.[42] However, the mechanistic borderline between the two reaction pathways in M^{n+}-promoted hydride-transfer reactions of NADH analogues has yet to be clarified, despite the important role of NADH in biological redox systems.

(21) Fukuzumi, S.; Ohkubo, K.; Tokuda, Y.; Suenobu, T. *J. Am. Chem. Soc.* **2000**, *122*, 4286.
(22) (a) Fukuzumi, S.; Ishikawa, M.; Tanaka, T. *J. Chem. Soc., Perkin Trans. 2* **1989**, 1037. (b) Fukuzumi, S.; Mochizuki, S.; Tanaka, T. *J. Am. Chem. Soc.* **1989**, *111*, 1497. (c) Fukuzumi, S.; Kitano, T.; Ishikawa, M. *J. Am. Chem. Soc.* **1990**, *112*, 5631.
(23) (a) Carlson, B. W.; Miller, L. L. *J. Am. Chem. Soc.* **1985**, *107*, 479. (b) Miller, L. L.; Valentine, J. R. *J. Am. Chem. Soc.* **1988**, *110*, 3982. (c) Colter, A. K.; Plank, P.; Bergsma, J. P.; Lahti, R.; Quesnel, A. A.; Parsons, A. G. *Can. J. Chem.* **1984**, *62*, 1780.
(24) (a) Coleman, C. A.; Rose, J. G.; Murray, C. J. *J. Am. Chem. Soc.* **1992**, *114*, 9755. (b) Murray, C. J.; Webb, T. *J. Am. Chem. Soc.* **1991**, *113*, 7426.
(25) (a) Sund, H. *Pyridine-Nucleotide Dependent Dehydrogenase*; Walter de Gruyer: West Berlin, 1977. (b) Kellog, R. M. *Top. Curr. Chem.* **1982**, *101*, 111. (c) Bunting, J. W. *Bioorg. Chem.* **1991**, *19*, 456. (d) He, G.-X.; Blasko, A.; Bruice, T. C. *Bioorg. Chem.* **1993**, *21*, 423. (e) Ohno, A. *J. Phys. Org. Chem.* **1995**, *8*, 567.
(26) (a) Sigman, D. S.; Hajdu, J.; Creighton, D. J. In *Bioorganic Chemistry*; van Tamelen, E. E., Ed.; Academic Press: New York, 1978; Vol. IV, p 385. (b) Gase, R. A.; Pandit, U. K. *J. Am. Chem. Soc.* **1979**, *101*, 7059.
(27) Fukuzumi, S.; Koumitsu, S.; Hironaka, K.; Tanaka, T. *J. Am. Chem. Soc.* **1987**, *109*, 305.
(28) (a) Ishikawa, M.; Fukuzumi, S. *J. Chem. Soc., Faraday Trans.* **1990**, *86*, 3531. (b) Fukuzumi, S.; Nishizawa, N.; Tanaka, T. *J. Chem. Soc., Perkin Trans. 2* **1985**, 371.
(29) (a) Fukuzumi, S.; Ohkubo, K.; Okamoto, T. *J. Am. Chem. Soc.* **2002**, *124*, 14147. (b) Fukuzumi, S.; Fujii, Y.; Suenobu, T. *J. Am. Chem. Soc.* **2001**, *123*, 10191.
(30) Fukuzumi, S.; Yuasa, J.; Suenobu, T. *J. Am. Chem. Soc.* **2002**, *124*, 12566.
(31) Reichenbach-Klinke, R.; Kruppa, M.; König, B. *J. Am. Chem. Soc.* **2002**, *124*, 12999.
(32) (a) Fukuzumi, S. *Bull. Chem. Soc. Jpn.* **1997**, *70*, 1. (b) Fukuzumi, S. In *Electron Transfer in Chemistry*; Balzani, V., Ed.; Wiley-VCH: Weinheim, 2001; Vol. 4, pp 3−67. (c) Fukuzumi, S. *Bull. Chem. Soc. Jpn.* **2006**, *79*, 177.
(33) Fukuzumi, S.; Yuasa, J.; Satoh, N.; Suenobu, T. *J. Am. Chem. Soc.* **2004**, *126*, 7585.
(34) (a) Fukuzumi, S.; Itoh, S. In *Advances in Photochemistry*; Neckers, D. C., Volman, D. H., von Bünau, G., Eds.; Wiley: New York, 1998; Vol. 25, pp 107−172. (b) Fukuzumi, S. *Org. Biomol. Chem.* **2003**, *1*, 609.
(35) Yuasa, J.; Suenobu, T.; Ohkubo, K.; Fukuzumi, S. *Chem. Commun.* **2003**, 1070.
(36) (a) Yuasa, J.; Suenobu, T.; Fukuzumi, S. *J. Am. Chem. Soc.* **2003**, *125*, 12090. (b) Yuasa, J.; Suenobu, T.; Fukuzumi, S. *ChemPhysChem* **2006**, *7*, 942.
(37) (a) Itoh, S.; Kawakami, H.; Fukuzumi, S. *J. Am. Chem. Soc.* **1998**, *120*, 7271. (b) Itoh, S.; Kawakami, H.; Fukuzumi, S. *J. Am. Chem. Soc.* **1997**, *119*, 439. (c) Itoh, S.; Kawakami, H.; Fukuzumi, S. *Biochemistry* **1998**, *37*, 6562.
(38) (a) Fukuzumi, S.; Okamoto, T.; Otera, J. *J. Am. Chem. Soc.* **1994**, *116*, 5503. (b) Fukuzumi, S.; Okamoto, T. *J. Am. Chem. Soc.* **1993**, *115*, 11600.
(39) Okamoto, K.; Imahori, H.; Fukuzumi, S. *J. Am. Chem. Soc.* **2003**, *125*, 7014.
(40) The example of metal ion complexes of *o*-semiquinone radical anions; see: (a) Ernst, S.; Hänel, P.; Jordanov, J.; Kaim, W.; Kasack, V.; Roth, E. *J. Am. Chem. Soc.* **1989**, *111*, 1733. (b) Rall, J.; Wanner, M.; Albrecht, M.; Hornung, F. M.; Kaim, W. *Chem.—Eur. J.* **1999**, *5*, 2802. (c) Schwederski, B.; Kasack, V.; Kaim, W.; Roth, E.; Jordanov, J. *Angew. Chem., Int. Ed. Engl.* **1990**, *29*, 78.
(41) Contact and separated ion pairs of alkali-metal salts of a nitrobenzene radical anion have been isolated and characterized by X-ray crystallography; see: (a) Lü, J.-M.; Rosokha, S. V.; Lindeman, S. V.; Neretin, I. S.; Kochi, J. K. *J. Am. Chem. Soc.* **2005**, *127*, 1797. (b) Davlieva, M. G.; Lü, J.-M.; Lindeman, S. V.; Kochi, J. K. *J. Am. Chem. Soc.* **2004**, *126*, 4557.

Scheme 2

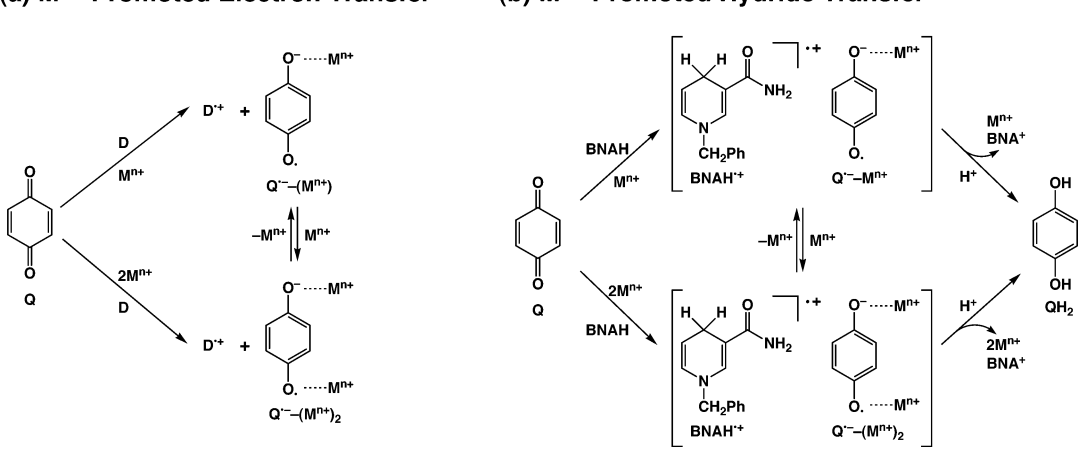

In this paper, we demonstrate the delicate balance between one-step hydride-transfer and electron-transfer pathways in a scandium ion (Sc^{3+})-promoted hydride-transfer reaction of an NADH analogue, 9,10-dihydro-10-methylacridine ($AcrH_2$), is changed by deuterium substitution of $AcrH_2$ by $AcrD_2$ and also by simple changes of temperature and Sc^{3+} concentration.[43] We have introduced a metal ion-binding site into *p*-benzoquinone to employ 1-(*p*-tolylsulfinyl)-2,5-benzoquinone (TolSQ) as a hydride acceptor. Sc^{3+}, which is one of the strongest Lewis acids among metal ions,[32] can form a complex with TolSQ, and this is the reason we chose Sc^{3+} to increase both electron- and hydride-acceptor abilities of TolSQ.[43] The TolSQ−Sc^{3+} complex is a common reactive intermediate in both Sc^{3+}-promoted hydride transfer from $AcrH_2$ to TolSQ and Sc^{3+}-promoted electron transfer from tris(2-phenylpyridine)iridium [$Ir(ppy)_3$][44] to TolSQ. The direct ESR detection of Sc^{3+} complexes of a semiquinone radical anion ($TolSQ^{\bullet-}$), combined with the kinetic analysis of Sc^{3+}-promoted electron-transfer and hydride-transfer reactions, provides valuable insight into the mechanistic borderline between one-step hydride-transfer and electron-transfer pathways as well as the mechanistic changeover in a Sc^{3+}-promoted hydride-transfer reaction of an NADH analogue for the first time.

Experimental Section

Materials. 1-(*p*-Tolylsulfinyl)-2,5-benzoquinone (TolSQ) was prepared according to the literature.[45] 9,10-Dihydro-10-methylacridine ($AcrH_2$) was synthesized by the reduction of 10-methylacridinium iodide ($AcrH^+I^-$) with $NaBH_4$ in methanol and purified by recrystallization from ethanol.[46] Synthesis of dideuterated 9,10-dihydro-10-methylacridine ($AcrD_2$) was described previously.[47] Tris(2-phenylpyridine)iridium [$Ir(ppy)_3$] was prepared according to the literature.[48] Scandium triflate [$Sc(OTf)_3$] (99%) was purchased from Pacific Metals Co., Ltd. (Taiheiyo Kinzoku). 10,10′-Dimethyl-9,9′-biacridine [$(AcrH)_2$] was prepared by the one-electron reduction of 10-methylacridinium perchlorate by hexamethylditin.[49a] Acetonitrile (MeCN) used as a solvent was purified and dried according to the standard procedure.[50] [$^2H_3$]Acetonitrile (CD_3CN) was obtained from EURI SO-TOP, CEA, France. [$^2H_2$]Water (D_2O) was purchased from Cambridge Isotope Laboratories. Tetra-*n*-butylammonium perchlorate (TBAP) was purchased from Fluka Chemical Co., twice recrystallized from absolute ethanol, and dried in a vacuum at 45 °C prior to use.

Reaction Procedures and Analysis. Typically, $AcrH_2$ (2.8×10^{-2} M) was added to an NMR tube that contained an [$^2H_3$]acetonitrile (CD_3CN) solution (0.6 mL) of TolSQ (1.0×10^{-2} M) in the presence of Sc^{3+} (3.0×10^{-2} M) under an atmospheric pressure of argon. Then the solution was deaerated with argon gas for 5 min, and the NMR tube was sealed with a rubber septum. The reaction was complete in 1 min under these conditions. The product of the hydride reduction of TolSQ, 1-(*p*-tolylsulfinyl)-2,5-benzohydroquinone ($TolSQH_2$), was identified by comparing the ^1H NMR spectra with those in the literatures.[51] The total yield of $TolSQH_2$ was determined to be 99% from the ^1H NMR spectra in comparison with the internal standard, 1,4-dioxane (7.1×10^{-2} M). ^1H NMR measurements were performed with a JMN-AL-300 (300 MHz) NMR spectrometer at 298 K. **TolSQH$_2$**: ^1H NMR (300 MHz, CD_3CN) in the presence of Sc^{3+} (3.0×10^{-2} M):[52] δ (ppm) 7.58 (d, $J = 8.3$ Hz, 2H), 7.33 (d, $J = 8.3$ Hz, 2H), 6.96 (d, $J = 2.9$ Hz, 1H), 6.80 (dd, $J = 2.9$ Hz, 8.4 Hz, 1H), 6.71 (d, $J = 8.4$ Hz, 1H), 2.37 (s, 3H).

Spectral Measurements. Formation of Sc^{3+} complexes of TolSQ [TolSQ−Sc^{3+}] was examined from the UV−vis spectral change of

(42) We have previously demonstrated that an electrophilicity of the carbonyl compound methyl vinyl ketone (MVK) is significantly increased by the complex formation with a scandium ion (Sc^{3+}), which enhances both the Diels−Alder reaction of anthracenes with MVK and photoinduced electron transfer from electron donors to MVK; see: Fukuzumi, S.; Yuasa, J.; Miyagawa, T.; Suenobu, T. *J. Phys. Chem. A* **2005**, *109*, 3174.
(43) The formation constants of other metal ion complexes of TolSQ were not large enough to be employed in this work.
(44) Cyclometalated Ir(III) complexes such as $Ir(ppy)_3$ have been used as outstanding phosphorescent materials for a wide variety of applications; see: (a) Holder, E.; Langeveld, B. M. W.; Schubert, U. S. *Adv. Mater.* **2005**, *17*, 1109. (b) Wang, X.-Y.; Prabhu, R. N.; Schmehl, R. H.; Weck, M. *Macromolecules* **2006**, *39*, 3140.
(45) (a) Grennberg, H.; Gogoll, A.; Bäckvall, J.-E. *J. Org. Chem.* **1991**, *56*, 5808. (b) Carreño, M. C.; García Ruano, J. L.; Urbano, A. *Tetrahedron Lett.* **1989**, *30*, 4003.
(46) Roberts, R. M. G.; Ostovic, D.; Kreevoy, M. M. *Faraday Discuss. Chem. Soc.* **1982**, *74*, 257.
(47) Fukuzumi, S.; Tokuda, Y.; Kitano, T.; Okamoto, T.; Otera, J. *J. Am. Chem. Soc.* **1993**, *115*, 8960.
(48) Dedeian, K.; Djurovich, P. I.; Garces, F. O.; Carlson, G.; Watts, R. J. *Inorg. Chem.* **1991**, *30*, 1685.
(49) (a) Fukuzumi, S.; Kitano, T.; Mochida, K. *J. Am. Chem. Soc.* **1990**, *112*, 3246. (b) Fukuzumi, S.; Tokuda, Y. *J. Phys. Chem.* **1992**, *96*, 8409.
(50) Armarego, W. L. F.; Perrin, D. D. *Purification of Laboratory Chemicals*, 4th ed.; Butterworth-Heinemann: Boston, 1996.
(51) (a) García Ruano, J. L.; Alemparte, C. *J. Org. Chem.* **2004**, *69*, 1405. (b) Carreño, M. C.; García Ruano, J. L.; Toledo, M. A.; Urbano, A. *Tetrahedron Lett.* **1994**, *35*, 9759. (c) Carreño, M. C.; García Ruano, J. L.; Lafuente, C.; Toledo, M. A. *Tetrahedron: Asymmetry* **1999**, *10*, 1119.
(52) Small amount of D_2O [in D_2O/CD_3CN (1:10, v/v)] was added to the CD_3CN solution of $TolSQH_2$ in order to avoid the coordination of Sc^{3+} to $TolSQH_2$.

TolSQ (1.0×10^{-3} M) at $\lambda = 343$ nm in the presence of various concentrations of Sc^{3+} [$(0-5.7) \times 10^{-3}$ M] by using a Hewlett-Packard 8453 diode array spectrophotometer.

Kinetic Measurements. Kinetic measurements were performed by using a UNISOKU RSP-601 stopped-flow spectrophotometer with an MOS-type high sensitive photodiode array. Rates of electron transfer from $Ir(ppy)_3$ (2.5×10^{-5} M) to TolSQ [$(0-2.5) \times 10^{-3}$ M] in the presence of Sc^{3+} [$(0-5.0) \times 10^{-2}$ M] were monitored by the rise and decay of the absorption band at 580 and 380 nm due to $[Ir(ppy)_3]^+$ and $Ir(ppy)_3$, respectively, in deaerated MeCN at 298 K. Rates of hydride transfer from $AcrH_2$ and $AcrD_2$ (3.0×10^{-5} M) to TolSQ [$(0-1.0) \times 10^{-3}$ M] in the presence of Sc^{3+} [$(0-5.0) \times 10^{-1}$ M] were monitored by an increase in the absorption band due to a 10-methylacridinium ion ($AcrH^+$: $\lambda_{max} = 358$ nm, $\epsilon_{max} = 1.80 \times 10^4$ M^{-1} cm^{-1}) in deaerated MeCN at 233−333 K in the dark. All kinetic measurements were carried out under pseudo-first-order conditions where the concentrations of TolSQ were maintained at more than 10-fold excess of the concentrations of $Ir(ppy)_3$ and $AcrH_2$ at 298 K. Pseudo-first-order rate constants were determined by least-squares curve fits using a personal computer.

Cyclic Voltammetry. Cyclic voltammetry measurements were performed on a ALS 630 A electrochemical analyzer in deaerated MeCN containing 0.1 M TBAP as a supporting electrolyte at 298 K. A conventional three-electrode cell was used with a platinum working electrode (surface area of 0.3 mm^2) and a platinum wire as the counter electrode. The Pt working electrode (BAS) was routinely polished with a BAS polishing alumina suspension and rinsed with acetone before use. The measured potentials were recorded with respect to the Ag/$AgNO_3$ (0.01 M) reference electrode. All potentials (vs Ag/Ag^+) were converted to values vs SCE by adding 0.29 V.[53] All electrochemical measurements were carried out under an atmospheric pressure of argon.

ESR Measurements. TolSQ (1.6×10^{-1} M) was dissolved in deaerated MeCN and purged with argon for 10 min. $Sc(OTf)_3$ (3.2×10^{-2} M in 1.0 mL) was dissolved in deaerated MeCN. The TolSQ (200 μL) and Sc^{3+} (200 μL) solutions were introduced into an ESR cell (1.8 mm i.d.) containing $(AcrH)_2$ (1.6×10^{-2} M) and mixed by bubbling with an Ar gas through a syringe with a long needle. The ESR spectra of the Sc^{3+} complexes with the semiquinone radical anion of TolSQ [$TolSQ^{\bullet-}-(Sc^{3+})$] and [$TolSQ^{\bullet-}-(Sc^{3+})_2$] were recorded on a JEOL JES-RE1XE spectrometer under irradiation of a high-pressure mercury lamp (USH-1005D) focusing at the sample cell in the ESR cavity at 298 K. The magnitude of modulation was chosen to optimize the resolution and signal-to-noise (*S*/*N*) ratio of the observed spectra under nonsaturating microwave power conditions. The *g* values were calibrated using a Mn^{2+} marker. Computer simulation of the ESR spectra was carried out by using Calleo ESR version 1.2 (Calleo Scientific Publisher) on a personal computer.

Results

Sc^{3+}-Promoted Hydride Transfer from $AcrH_2$ to TolSQ. 1-(*p*-Tolylsulfinyl)-2,5-benzoquinone (TolSQ) forms a 1:1 complex with the scandium ion (eq 1) as indicated by UV−vis spectral changes of TolSQ in the presence of various concentrations of $Sc(OTf)_3$ [OTf = OSO_2CF_3] in acetonitrile (MeCN) at 298 K as shown in Figure 1.[54] Such an absorbance change due

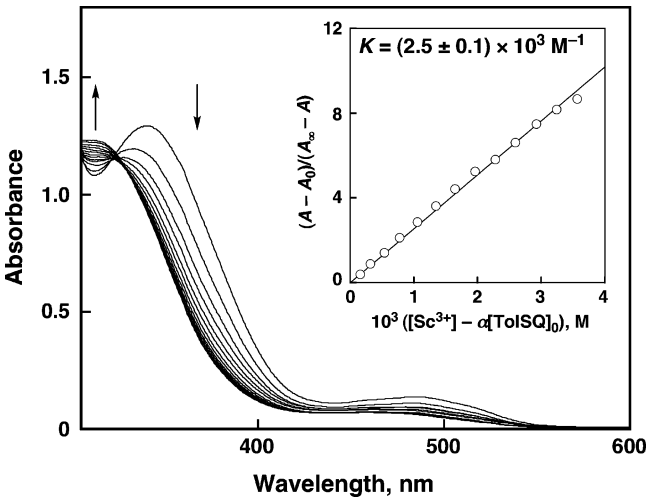

Figure 1. UV−vis absorption spectra of TolSQ (1.0×10^{-3} M) in the presence of Sc^{3+} [$(0-5.7) \times 10^{-3}$ M] in MeCN at 298 K. Inset: Plot of $(A - A_0)/(A_\infty - A)$ vs $[Sc^{3+}] - \alpha[TolSQ]_0$, where $\alpha = (A - A_0)/(A_\infty - A_0)$ at $\lambda = 343$ nm.

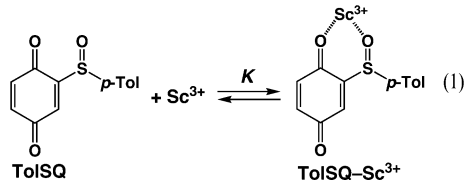

to the complex formation between TolSQ and Sc^{3+} is expressed by eq 2, where A_0 and A_∞ are absorbance due to TolSQ and absorbance due to the TolSQ−Sc^{3+} complex at 343 nm, and $[TolSQ]_0$ denotes the initial concentration of TolSQ. The formation constant (K) is determined as $(2.5 \pm 0.1) \times 10^3$ M^{-1} from a linear plot of $(A - A_0)/(A_\infty - A)$ vs $([Sc^{3+}] - \alpha[TolSQ]_0)$ [$\alpha = (A - A_0)/(A_\infty - A_0)$]; see inset of Figure 1.

$$(A - A_0)/(A_\infty - A) = K\{[Sc^{3+}] - \alpha[TolSQ]_0\} \qquad (2)$$

Hydride transfer from an NADH analogue, 9,10-dihydro-10-methylacridine ($AcrH_2$), to TolSQ is expected to be accelerated by the complex formation of TolSQ with Sc^{3+}. In fact, hydride transfer from $AcrH_2$ to TolSQ occurs efficiently in the presence of Sc^{3+} to yield the 10-methylacridinium ion ($AcrH^+$) and 1-(*p*-tolylsulfinyl)-2,5-benzohydroquinone ($TolSQH_2$) in deaerated MeCN at 298 K (eq 3; for the product analysis, see Experimental Section), whereas no hydride-transfer reaction has occurred in the absence of Sc^{3+}. The spectral titration of $AcrH_2$ by TolSQ

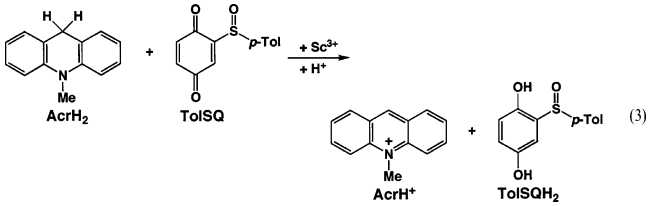

was examined in order to confirm the stoichiometry in eq 3 (Figure 2). The ratio of the $AcrH^+$ concentration to the initial concentration of $AcrH_2$ ($[AcrH^+]/[AcrH_2]_0$) is plotted against the ratio of the TolSQ concentration to the initial concentration of $AcrH_2$ ($[TolSQ]/[AcrH_2]_0$). All $AcrH_2$ molecules are consumed by the addition of 1 equiv of TolSQ to yield 1 equiv of

(53) Mann, C. K.; Barnes, K. K. *Electrochemical Reactions in Nonaqueous Systems*; Marcel Dekker: New York, 1990.

(54) The complex formation between TolSQ (2.0×10^{-2} M) and Sc^{3+} was also confirmed by the ^1H and ^{13}C NMR. ^1H NMR (300 MHz, CD_3CN) in the absence of Sc^{3+}: δ (ppm) 7.65 (d, $J = 8.1$ Hz, 2H), 7.35 (d, $J = 8.1$ Hz, 2H), 7.24 (d, $J = 2.4$ Hz, 1H), 6.82 (dd, $J = 2.4$ Hz, 10.1 Hz, 1H), 6.73 (d, $J = 10.1$ Hz, 1H), 2.38 (s, 3H). ^1H NMR (300 MHz, CD_3CN) in the presence of Sc^{3+} (6.0×10^{-2} M): δ (ppm) 7.77 (d, $J = 8.7$ Hz, 2H), 7.52 (d, $J = 2.2$ Hz, 1H), 7.44 (d, $J = 8.7$ Hz, 2H), 6.92 (dd, $J = 2.2$ Hz, 10.1 Hz, 1H), 6.82 (d, $J = 10.1$ Hz, 1H), 2.42 (s, 3H). ^{13}C NMR (300 MHz, CD_3CN) in the absence of Sc^{3+}: δ (ppm) 186.6, 185.2, 155.8, 144.3, 140.1, 138.7, 137.5, 132.9, 131.2, 127.3, 21.5. ^{13}C NMR (300 MHz, CD_3CN) in the presence of Sc^{3+} (6.0×10^{-2} M): δ (ppm) 185.5, 184.1, 147.8, 147.6, 139.3, 137.1, 135.0, 132.4, 131.9, 129.4, 21.8.

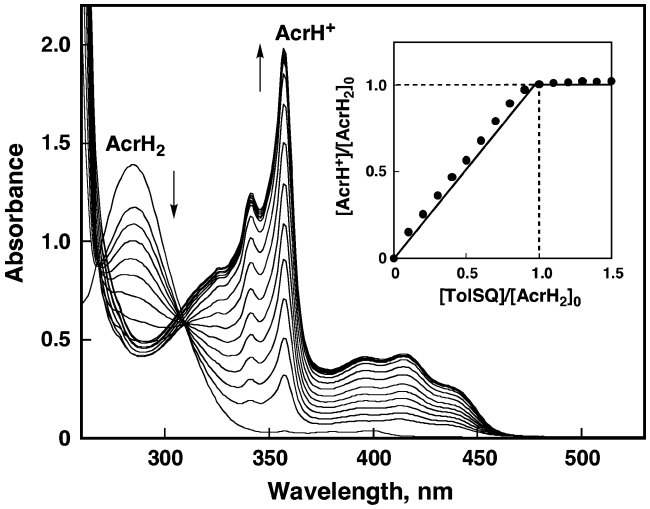

Figure 2. Absorption spectral changes observed upon addition of TolSQ [(0−1.5) × 10^{-4} M] to a deaerated MeCN solution of $AcrH_2$ (1.0 × 10^{-4} M) in the presence of Sc^{3+} (1.0 × 10^{-2} M) at 298 K. Inset: Plot of the ratio of the $AcrH^+$ concentration to the initial concentration of $AcrH_2$ (1.0 × 10^{-4} M), $[AcrH^+]/[AcrH_2]_0$, vs the ratio of the TolSQ concentration to the initial concentration of $AcrH_2$, $[TolSQ]/[AcrH_2]_0$.

$AcrH^+$ (λ_{max} = 358 nm, $\epsilon_{max} = 1.80 \times 10^4\ M^{-1}\ cm^{-1}$) as shown in the inset of Figure 2.[55,56]

Rates of hydride transfer from $AcrH_2$ to TolSQ in the presence of Sc^{3+} were determined by monitoring an increase in the absorption band due to $AcrH^+$ in deaerated MeCN. The rates obeyed pseudo-first-order kinetics in the presence of a large excess of TolSQ and Sc^{3+} relative to the concentration of $AcrH_2$ (see the first-order plots in Supporting Information S1). The observed pseudo-first-order rate constants (k_{obs}) increase proportionally with TolSQ concentration (see Supporting Information S2). Thus, the rate exhibits a second-order kinetics showing a first-order dependence on each reactant concentration.

The dependence of the observed second-order rate constant (k_H) on $[Sc^{3+}]$ was examined for hydride transfer from $AcrH_2$ to TolSQ at various concentrations of Sc^{3+} as shown in Figure 3a (red closed circles). The k_H value increases with increasing Sc^{3+} concentration to reach a constant value ($k_H = 1.4 \times 10^3\ M^{-1}\ s^{-1}$). The rates of hydride transfer exhibit a large primary kinetic deuterium isotope effect ($k_H/k_D = 5.3 \pm 0.1$) at low concentrations ($[Sc^{3+}] < 1.0 \times 10^{-2}$ M) when $AcrH_2$ is replaced by the dideuterated compound ($AcrD_2$). In contrast to the case of $AcrH_2$, the observed second-order rate constant (k_D) increases linearly with an increase in $[Sc^{3+}]$ without exhibiting a saturation behavior at high concentrations ($[Sc^{3+}] > 1.0 \times 10^{-2}$ M) as shown in Figure 3a (blue closed circles). The primary kinetic deuterium isotope effect (k_H/k_D) therefore decreases with increasing $[Sc^{3+}]$ at high concentrations ($[Sc^{3+}] > 1.0 \times 10^{-2}$ M).[57] The dependence of the observed second-order rate constants (k_H and k_D) on $[Sc^{3+}]$ are changed drastically when the temperature is lowered to 233 K, where both k_H and k_D values increase linearly with increasing $[Sc^{3+}]$, exhibiting a

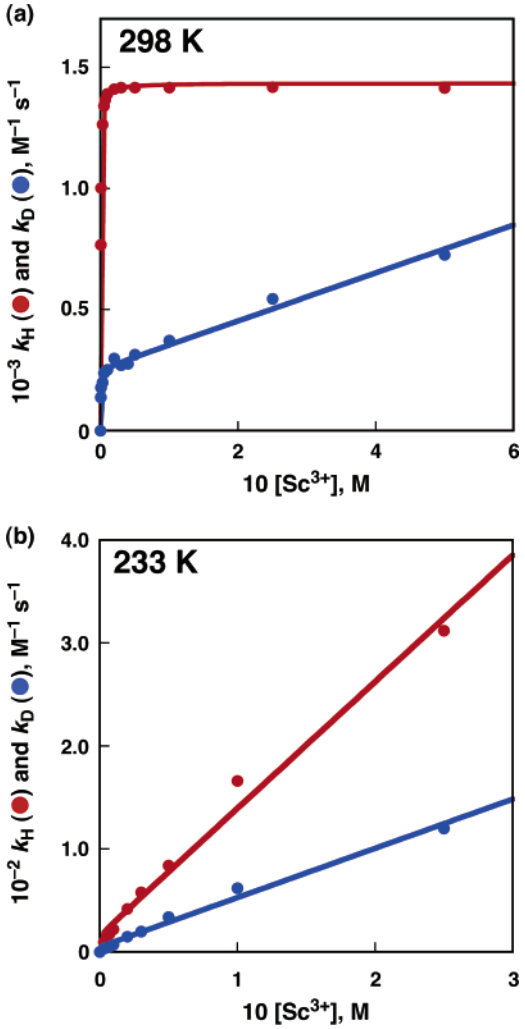

Figure 3. Dependence of k_H (red closed circle) and k_D (blue closed circle) on $[Sc^{3+}]$ for hydride transfer from $AcrH_2$ (3.0 × 10^{-5} M) and $AcrD_2$ (3.0 × 10^{-5} M) to TolSQ in the presence of Sc^{3+} in deaerated MeCN at (a) 298 K and (b) 233 K.

primary kinetic deuterium isotope effect ($k_H/k_D = 2.6 \pm 0.2$) irrespective of Sc^{3+} concentration as shown in Figure 3b (red and blue closed circles, respectively).

The remarkable change with regard to the dependence of the rate constant of hydride transfer on $[Sc^{3+}]$ by deuterium substitution of $AcrH_2$ by $AcrD_2$, and also by simple change of temperature indicates a mechanistic changeover in the hydride-transfer reaction. In such a case, a temperature dependence of rates of the hydride-transfer reactions would provide valuable insight into the mechanistic changeover in the hydride-transfer reaction: one-step hydride transfer and electron transfer followed by proton−electron transfer. Thus, we examined the temperature dependence of rates of hydride-transfer reactions of $AcrH_2$ and $AcrD_2$ in the presence of high and low concentrations of Sc^{3+} (2.5 × 10^{-1} M and 1.0 × 10^{-2} M, respectively).[58]

A plot of ln k_H vs T^{-1} for the hydride-transfer reaction of $AcrH_2$ in the presence of a high concentration of Sc^{3+} (2.5 × 10^{-1} M) is shown in Figure 4a (red open circles), where there are two segments in the temperature range 233−298 K and 298−333 K with clearly different slopes. In contrast, a single

(55) There is no isosbestic point in the spectral titration of $AcrH_2$ by TolSQ after the 1:1 ratio of TolSQ to $AcrH_2$, since the absorption band due to an excess of TolSQ−Sc^{3+} is overlapped with the isosbestic points (269 and 310 nm).
(56) The source of a proton in eq 3 is a small amount of water (6.5 mM) contained in MeCN.
(57) The k_D values at higher concentrations of Sc^{3+} ($[Sc^{3+}] > 0.5$ M) could not be determined because $Sc(OTf)_3$ was not soluble in MeCN at higher concentrations.
(58) Almost all TolSQ molecules form the TolSQ−Sc^{3+} complex under these conditions.

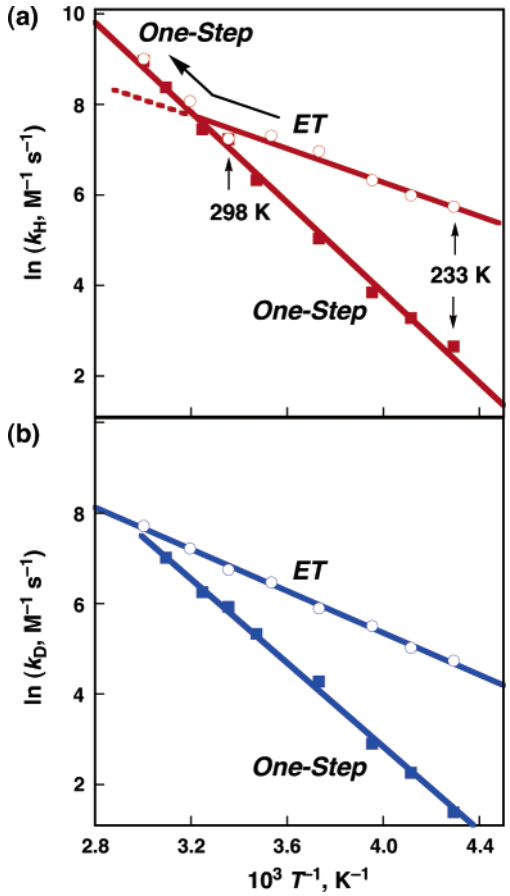

Figure 4. (a) Plots of ln k_H vs T^{-1} for hydride transfer from $AcrH_2$ (3.0×10^{-5} M) to TolSQ in the presence of $Sc(OTf)_3$ (1.0×10^{-2} M: red closed square, 2.5×10^{-1} M: red open circle) in deaerated MeCN. (b) Plots of ln k_D vs T^{-1} for hydride transfer from $AcrD_2$ (3.0×10^{-5} M) to TolSQ in the presence of $Sc(OTf)_3$ (1.0×10^{-2} M: blue closed square, 2.5×10^{-1} M: blue open circle) in deaerated MeCN.

linear correlation is observed between ln k_H and T^{-1} for the hydride-transfer reaction of $AcrH_2$ in the presence of a low concentration of Sc^{3+} (1.0×10^{-2} M: red closed squares in Figure 4a). In consequence, the k_H value in the presence of a high concentration of Sc^{3+} (2.5×10^{-1} M: red open circles) increases with increasing temperature to merge into the k_H values in the presence of a low concentration of Sc^{3+} (1.0×10^{-2} M: red closed squares). Thus, even though the k_H value in the presence of a high concentration of Sc^{3+} (2.5×10^{-1} M: $k_H = 3.1 \times 10^2$ M^{-1} s^{-1}) is 23 times larger than the k_H value in the presence of a low concentration of Sc^{3+} (1.0×10^{-2} M: $k_H = 1.4 \times 10^1$ M^{-1} s^{-1}) at 233 K, the k_H values in the presence of high and low concentrations of Sc^{3+} (2.5×10^{-1} M: red open circles and 1.0×10^{-2} M: closed squares, respectively) become virtually the same in the temperature range 298−333 K (see the first-order plots at 333 and 233 K in Supporting Information S1). In contrast with the case of k_H in Figure 4a, single linear correlations are observed between ln k_D and T^{-1} for the hydride-transfer reactions of $AcrD_2$ in the presence of both low and high concentrations of Sc^{3+} (1.0×10^{-2} M and 2.5×10^{-1} M) as shown in Figure 4b (blue closed squares and open circles, respectively). Such differences in the temperature dependence of k_H and k_D depending on concentrations of Sc^{3+} result from the changeover of the reaction pathways as discussed later.

Scandium Ion-Promoted Electron Transfer from Ir(ppy)$_3$ to TolSQ. When $AcrH_2$ is replaced by tris(2-phenylpyridine)-iridium [$Ir(ppy)_3$],[48] which is used as an electron donor, no electron transfer from $Ir(ppy)_3$ ($E°_{ox}$ vs SCE = 0.71 V) to TolSQ ($E°_{red}$ vs SCE = −0.26 V) occurs in the absence of Sc^{3+}, because the free energy change of electron transfer is largely positive ($\Delta G_{et} = 0.97$ eV). The $E°_{ox}$ value of $Ir(ppy)_3$ and the $E°_{red}$ value of TolSQ were determined by cyclic voltammetry measurements (see Supporting Information S3).

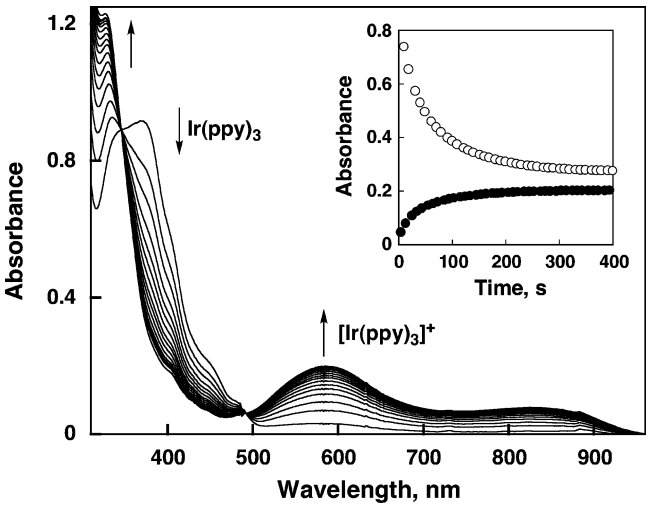

Figure 5. Absorption spectral changes observed in electron transfer from $Ir(ppy)_3$ (5.0×10^{-5} M) to TolSQ (5.0×10^{-5} M) in the presence of Sc^{3+} (3.0×10^{-4} M) in deaerated MeCN at 298 K. Inset: Time course of absorption changes at $\lambda = 380$ nm (○) and 580 nm (●).

Upon addition of $Sc(OTf)_3$ (3.0×10^{-4} M) to a deaerated MeCN solution of $Ir(ppy)_3$ (5.0×10^{-5} M) and TolSQ (5.0×10^{-5} M), however, electron transfer from $Ir(ppy)_3$ ($\lambda_{max} = 380$ nm) to TolSQ occurs efficiently to yield $[Ir(ppy)_3]^+$ ($\lambda_{max} = 580$ nm) as shown in Figure 5 (eq 4). The one-electron reduction

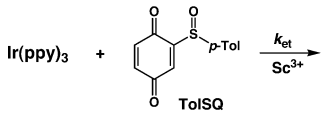

$$[Ir(ppy)_3]^+ + TolSQ^{\bullet-}\text{–}(Sc^{3+})_n \quad (n = 1, 2) \qquad (4)$$

potential of TolSQ (E_{red}) in the presence of Sc^{3+} is shifted to the positive direction due to the complex formation of $TolSQ^{\bullet-}$ with Sc^{3+} according to the Nernst equation (eq 5),[59] where $E°_{red}$ is the one-electron reduction potential of TolSQ in the absence of Sc^{3+}, and K_1 and K_2 are the formation constant of $TolSQ^{\bullet-}$–Sc^{3+} and $TolSQ^{\bullet-}$–$(Sc^{3+})_2$, respectively.

$$E_{red} = E°_{red} + (2.3RT/F) \log\{(1 + K_1[Sc^{3+}])(1 + K_2[Sc^{3+}])/(1 + K[Sc^{3+}])\} \qquad (5)$$

For example, the reduction potential of TolSQ is shifted to 0.70 V in the presence of 1.0 M Sc^{3+} (see Supporting Information S4).[60]

The rates obeyed pseudo-first-order kinetics in the presence of a large excess TolSQ and Sc^{3+} relative to the concentration of $Ir(ppy)_3$ (see the first-order plot in Supporting Information S5). The observed pseudo-first-order rate constant (k_{obs})

(59) Bard, A. J.; Faulkner, L. R. *Electrochemical Methods, Fundamentals and Applications*; John Wile & Sons: New York, 1980.
(60) In contrast to the one-electron reduction of TolSQ, the one-electron oxidation potential of $Ir(ppy)_3$ was hardly affected by the presence of Sc^{3+}.

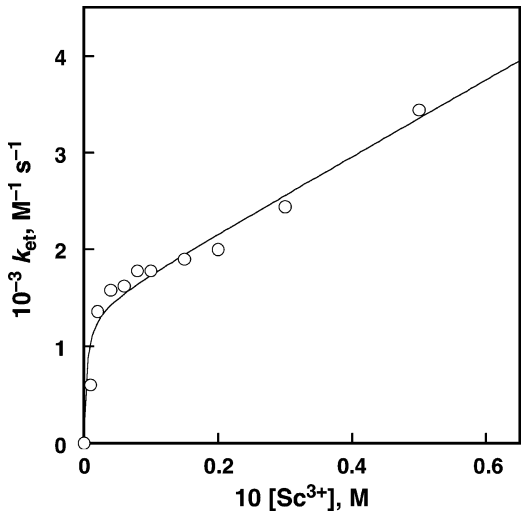

Figure 6. Dependence of k_{et} on [Sc^{3+}] for electron transfer from $Ir(ppy)_3$ (2.5×10^{-5} M) to TolSQ in the presence of Sc^{3+} in deaerated MeCN at 298 K.

increases proportionally with increasing TolSQ concentration (see Supporting Information S6). The second-order rate constant of electron transfer (k_{et}) exhibits a saturated dependence on [Sc^{3+}] at low concentrations of Sc^{3+} ([Sc^{3+}] < 1.0×10^{-2} M) as shown in Figure 6. The saturated dependence of k_{et} on [Sc^{3+}] is changed to a first-order dependence on [Sc^{3+}] at high concentrations ([Sc^{3+}] > 1.0×10^{-2} M) as in the case of the hydride-transfer reaction of $AcrD_2$ (blue closed circles in Figure 3a).

ESR Detection of the Sc^{3+} Complex of $TolSQ^{\bullet-}$. A Sc^{3+} complex of the semiquinone radical anion of TolSQ ($TolSQ^{\bullet-}$) should be a key intermediate in Sc^{3+}-promoted electron transfer from $Ir(ppy)_3$ to TolSQ as well as Sc^{3+}-promoted hydride transfer from $AcrH_2$ to TolSQ. The $TolSQ^{\bullet-}$ and the Sc^{3+} complex were detected by ESR as follows.

$TolSQ^{\bullet-}$ was produced by photoinduced electron transfer from the 10,10′-dimethyl-9,9′-biacridine [$(AcrH)_2$] to TolSQ in deaerated MeCN at 298 K (Scheme 3). The $(AcrH)_2$ is known to act as an electron donor in contrast with the case of the monomer, $AcrH_2$, which is a hydride donor.[49] The ESR spectrum of $TolSQ^{\bullet-}$ is shown in Figure 7a together with the computer simulation spectrum with the hyperfine coupling constants [*hfc*: $a(H) = 2.00$ G, $a(H) = 2.20$ G, and $a(H) = 3.35$ G] in Figure 7b.

The addition of a small amount of $Sc(OTf)_3$ (1.6×10^{-2} M) to the $(AcrH)_2$−TolSQ system results in a drastic change in the hyperfine pattern of $TolSQ^{\bullet-}$ due to the complexation with Sc^{3+} (Scheme 3) as shown in Figure 7c. The ESR spectrum is well reproduced by the computer simulation spectrum with the *hfc* values of $a(2H) = 1.85$, 0.69 G and superhyperfine splitting due to one Sc^{3+} ion [$a(Sc^{3+}) = 1.69$ G] (Figure 7d). The complete agreement of the observed ESR spectrum (Figure 7c) with the computer simulation spectrum (Figure 7d) indicates that $TolSQ^{\bullet-}$ forms a 1:1 complex with Sc^{3+} ($TolSQ^{\bullet-}$−Sc^{3+}) in the presence of low concentrations of Sc^{3+} (1.6×10^{-2} M).[61,62] Upon addition of a large amount of $Sc(OTf)_3$ (4.6×10^{-1} M) to the $(AcrH)_2$−TolSQ−Sc^{3+} system, a drastic change in the hyperfine pattern of $TolSQ^{\bullet-}$−Sc^{3+} due to further superhyperfine splitting due to an additional Sc^{3+} ion is observed (Figure 7e).[62] This indicates that the $TolSQ^{\bullet-}$−Sc^{3+} complex is converted to a 1:2 complex with Sc^{3+} [$TolSQ^{\bullet-}$−$(Sc^{3+})_2$] at a high concentration of Sc^{3+} (4.6×10^{-1} M) as shown in Scheme 3.

The *g* values of the $TolSQ^{\bullet-}$−$(Sc^{3+})_2$ complex (2.0045) is smaller than that of the $TolSQ^{\bullet-}$−Sc^{3+} complex (2.0048) and free $TolSQ^{\bullet-}$ (2.0057). The smaller *g* value of the $TolSQ^{\bullet-}$−$(Sc^{3+})_2$ complex than that of the $TolSQ^{\bullet-}$−Sc^{3+} complex (2.0048) and free $TolSQ^{\bullet-}$ (2.0057) indicates that the spin density on oxygen nuclei in $TolSQ^{\bullet-}$ is significantly decreased by the binding with two Sc^{3+} ions.

Discussion

We wish to discuss how the mechanistic changeover, i.e., one-step hydride transfer (H^-) vs electron transfer followed by proton−electron transfer ($e^- + H^+ + e^-$) in the Sc^{3+}-promoted hydride-transfer reactions of $AcrH_2$ and $AcrD_2$ with TolSQ, results in the change in the dependence of k_H and k_D on [Sc^{3+}] with temperature (Figure 3 and Figure 4) by comparing the Sc^{3+}-promoted hydride-transfer reaction with the Sc^{3+}-promoted electron transfer from $Ir(ppy)_3$ to TolSQ (Figure 6).

Reactive Intermediate in Sc^{3+}-Promoted Hydride Transfer from $AcrH_2$ to TolSQ. The saturated dependence of k_H of a hydride transfer from $AcrH_2$ to TolSQ (red closed circles in Figure 3a) on [Sc^{3+}] is ascribed to the 1:1 complex formation between TolSQ and Sc^{3+} (TolSQ−Sc^{3+}). Formation of the TolSQ−Sc^{3+} complex is confirmed by UV−vis spectral changes of TolSQ in the presence of various concentrations of Sc^{3+} (Figure 1). When hydride transfer from $AcrH_2$ to TolSQ proceeds via the TolSQ−Sc^{3+} complex as shown in Scheme 4,[63] the dependence of k_H on [Sc^{3+}] is expressed by eq 6, which is rewritten by a linear relation between k_H^{-1} and [Sc^{3+}]$^{-1}$ (eq 7).

$$k_H = k^\circ_H K[Sc^{3+}]/(1 + K[Sc^{3+}]) \quad (6)$$

$$k_H^{-1} = \{k^\circ_H K[Sc^{3+}]\}^{-1} + k^\circ_H{}^{-1} \quad (7)$$

From the slope and intercepts of the linear plot of k_H^{-1} vs [Sc^{3+}]$^{-1}$ (see Supporting Information S7) are obtained the k°_H and *K* values of 1.4×10^3 M^{-1} s^{-1} and $(2.3 \pm 0.1) \times 10^3$ M^{-1}, respectively. The *K* values derived from the Sc^{3+}-promoted hydride-transfer reaction of $AcrH_2$ [$(2.3 \pm 0.1) \times 10^3$ M^{-1}] agrees with that determined from UV−vis spectral changes of TolSQ in the presence of various concentrations of Sc^{3+} [$K = (2.5 \pm 0.1) \times 10^3$ M^{-1}] at 298 K. Such agreement indicates that the TolSQ−Sc^{3+} complex is indeed a reactive intermediate in the Sc^{3+}-promoted hydride transfer from $AcrH_2$ to TolSQ as shown in Scheme 4. In contrast with the case of $AcrH_2$, the k_D value of $AcrD_2$ increases linearly with increasing Sc^{3+} concentration without exhibiting any saturation behavior at 298 K, although most TolSQ molecules form the Sc^{3+}

(61) Examples of the 1:1 complex formation between semiquinone radical anions with metal ions; see: ref 36b.

(62) A small amount of water was added to a deaerated MeCN solution of the $(AcrH)_2$−TolSQ system to obtain the high-resolution hyperfine structures of the $TolSQ^{\bullet-}$−Sc^{3+} and $TolSQ^{\bullet-}$−$(Sc^{3+})_2$ complexes, when self-exchange electron transfer with neutral TolSQ, which results in an increase in the line width, is slowed; see: ref 36b.

(63) $TolSQH^-$ and $TolSQH_2$ may interact with Sc^{3+}, because even TolSQ (the oxidized form) that is less electron rich than $TolSQH^-$ and $TolSQH_2$ can form a complex with Sc^{3+} (Scheme 4) via a metal-ion binding site (carbonyl oxygen or sulfinyl oxygen). However, the complex formation of $TolSQH^-$ and $TolSQH_2$ with Sc^{3+} has yet to be confirmed.

Scheme 3

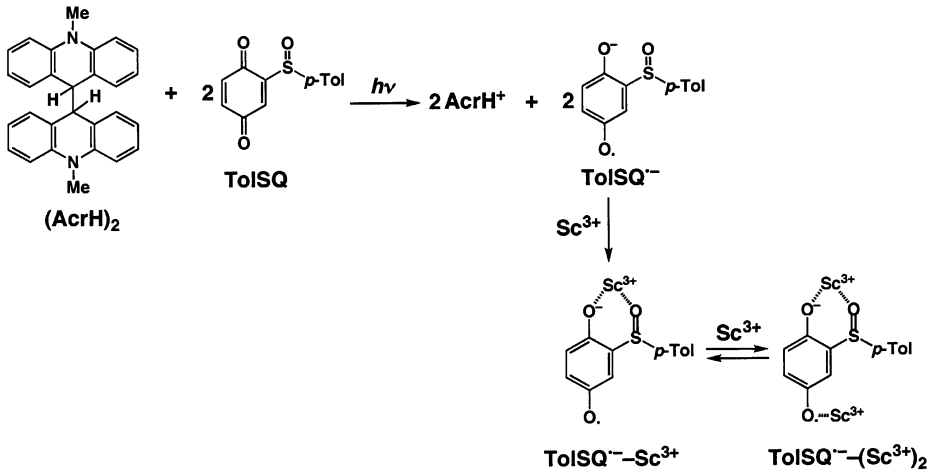

complex in the high concentration range in Figure 3a (blue closed circles). At a lower temperature (233 K), both the k_H and k_D values increase linearly with increasing [Sc^{3+}] without exhibiting any saturation behavior (Figure 3b), although the formation constant of the TolSQ−Sc^{3+} complex becomes much larger at 233 K [$K = (9.7 \pm 0.1) \times 10^3$ M^{-1}; see Supporting Information S8]. Such a linear dependence of k_H and k_D on [Sc^{3+}] cannot be explained by one-step hydride transfer from $AcrH_2$ and $AcrD_2$ to the TolSQ−Sc^{3+} complex in Scheme 4. In the case of Sc^{3+}-promoted electron transfer, however, the rate of electron transfer increases linearly with increasing [Sc^{3+}] as discussed below.

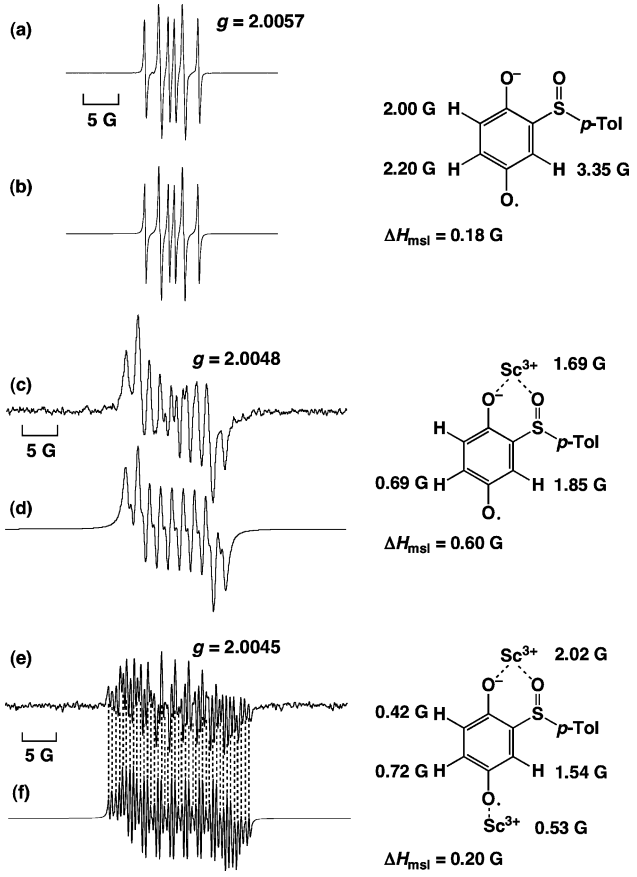

Figure 7. (a) ESR spectrum of TolSQ•− produced by photoinduced electron transfer from $(AcrH)_2$ (1.6×10^{-2} M) to TolSQ (1.0×10^{-3} M) in deaerated MeCN at 298 K and (b) the computer simulation spectrum. (c) ESR spectrum of TolSQ•−Sc^{3+} produced by photoinduced electron transfer from $(AcrH)_2$ (1.6×10^{-2} M) to TolSQ (8.0×10^{-2} M) in the presence of Sc^{3+} (1.6×10^{-2} M) and H_2O (2.2 M) in deaerated MeCN at 298 K and (d) the computer simulation spectrum. (e) ESR spectrum of TolSQ•−$(Sc^{3+})_2$ produced by photoinduced electron transfer from $(AcrH)_2$ (1.6×10^{-2} M) to TolSQ (4.6×10^{-2} M) in the presence of Sc^{3+} (4.6×10^{-1} M) and H_2O (4.4 M) in deaerated MeCN at 298 K and (f) the computer simulation spectrum.

Mechanism of Sc^{3+}-Promoted Electron Transfer from Ir(ppy)$_3$ to TolSQ. The saturated dependence of k_{et} of Sc^{3+}-promoted electron transfer from Ir(ppy)$_3$ to TolSQ on [Sc^{3+}] at low concentrations of Sc^{3+} ([Sc^{3+}] < 1.0×10^{-2} M) in Figure 6 indicates that the electron-transfer proceeds via the TolSQ−Sc^{3+} complex to produce the TolSQ•−−Sc^{3+} complex.[64] The TolSQ•−−Sc^{3+} complex was detected by ESR (Figure 7c). The first-order dependence of k_{et} on [Sc^{3+}] at high concentrations ([Sc^{3+}] > 1.0×10^{-2} M) in Figure 6 indicates that an additional Sc^{3+} ion is involved in the electron transfer to produce a 1:2 complex of TolSQ•− with Sc^{3+} [TolSQ•−−$(Sc^{3+})_2$] as shown in Scheme 5. The produced TolSQ•−−$(Sc^{3+})_2$ complex was also directly detected by ESR (Figure 7e).

According to Scheme 5, the dependence of k_{et} on [Sc^{3+}] is expressed by eq 8, which is rewritten by a linear correlation between $k_{et}(1 + K[Sc^{3+}])/(K[Sc^{3+}])$ and [Sc^{3+}] (eq 9),

$$k_{et} = (k_1 + k_2[Sc^{3+}])K[Sc^{3+}]/(1 + K[Sc^{3+}]) \quad (8)$$

$$k_{et}(1 + K[Sc^{3+}])/(K[Sc^{3+}]) = k_1 + k_2[Sc^{3+}] \quad (9)$$

where k_1 and k_2 are the rate constant of electron transfer to produce TolSQ•−−Sc^{3+} and TolSQ•−−$(Sc^{3+})_2$, respectively. From the intercept and slope, the k_1 and k_2 values are determined as $(1.2 \pm 0.1) \times 10^3$ M^{-1} s^{-1} and $(4.5 \pm 0.4) \times 10^4$ M^{-2} s^{-1}, respectively (Supporting Information S9). The dependence of k_{et} on [Sc^{3+}] can be fitted by eq 8 using the k_1 and k_2 values as shown in Figure 6 (solid line). Such dependence of k_{et} on [Sc^{3+}] is diagnostic of Sc^{3+}-promoted electron-transfer reduction of TolSQ to produce not only the 1:1 complex (TolSQ•−−Sc^{3+}) but also the 1:2 complex [TolSQ•−−$(Sc^{3+})_2$]. The k_2/k_1 ratio is 38 ± 6 M^{-1} that corresponds to the formation constant of

(64) The K value could not be determined actually by the dependence of k_{et} on [Sc^{3+}], because the k_{et} value increases linearly with increasing Sc^{3+} concentration at high concentrations of Sc^{3+}.

Scheme 4

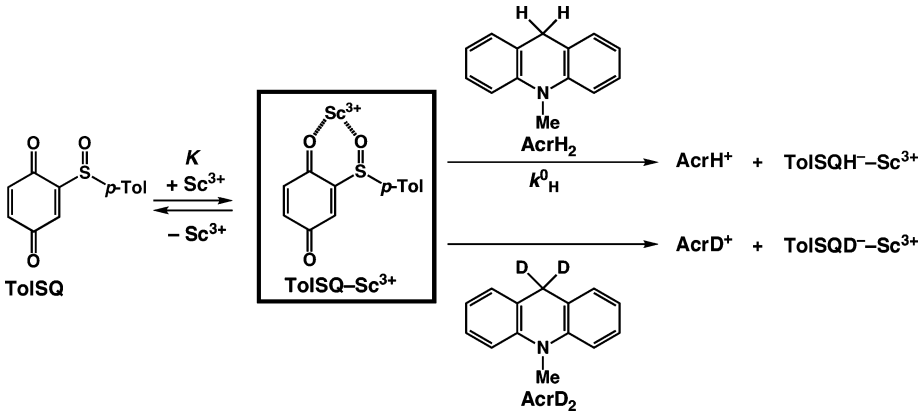

Scheme 5

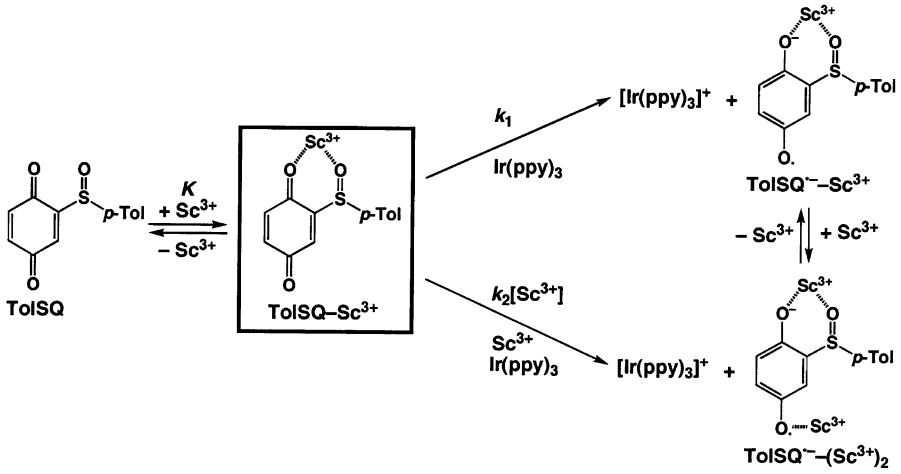

$TolSQ^{\bullet-}-(Sc^{3+})_2$ (K_2) from $TolSQ^{\bullet-}-Sc^{3+}$. The log K_1 value for the $TolSQ^{\bullet-}-Sc^{3+}$ complex is determined as 18.1 from the positive shift of the E_{red} value (0.96 V) in the presence of 1.0 M Sc^{3+} using eq 5 with the K value (2.5×10^3 M^{-1}) for the $TolSQ-Sc^{3+}$ complex and K_2 value (38 ± 6 M^{-1}) for the $TolSQ^{\bullet-}-(Sc^{3+})_2$ complex.[65] The E_{red} value in the presence of 3.0×10^{-4} M Sc^{3+} is estimated as 0.59 V using eq 5 with K, K_1, and K_2 values. In such a case, electron transfer from Ir(ppy)$_3$ ($E_{ox} = 0.71$ V) to TolSQ ($E_{red} = 0.59$ V) is expected to be slightly uphill. However, the follow-up disproportionation of the $TolSQ^{\bullet-}-Sc^{3+}$ complex makes the one-electron oxidation of Ir(ppy)$_3$ undergo to completion (Figure 5). The k_{et} values in Figure 6 have been determined under the pseudo-first-order conditions such that concentrations of TolSQ and Sc^{3+} are in large excess compared to that of Ir(ppy)$_3$, when the electron-transfer equilibrium may lie toward the products.

One-Step Hydride Transfer vs Electron Transfer Followed by Proton−Electron Transfer. The hydride transfer from $AcrH_2$ to the $TolSQ-Sc^{3+}$ complex at 298 K may occur via one-step hydride transfer as indicated by the saturated dependence of k_H on [Sc^{3+}] (red closed circles in Figure 3a). In contrast, the k_D value of $AcrD_2$ increases linearly with increasing [Sc^{3+}] at high concentrations ([Sc^{3+}] > 1.0×10^{-2} M) without exhibiting any saturation behavior (blue closed circles in Figure 3a). Such dependence of k_D on [Sc^{3+}] in Figure 3a is virtually the same as that observed in the Sc^{3+}-promoted electron-transfer reduction of TolSQ (Figure 6). Thus, the hydride-transfer mechanism may be changed from one-step hydride transfer from $AcrH_2$ to the $TolSQ-Sc^{3+}$ complex to Sc^{3+}-promoted electron transfer from $AcrD_2$ to the $TolSQ-Sc^{3+}$ complex as shown in Scheme 6a.

The dependence of the rate constant of Sc^{3+}-promoted electron transfer (k_{et}) from $AcrD_2$ to the $TolSQ-Sc^{3+}$ complex can be estimated from the dependence of k_{et} of Sc^{3+}-promoted electron transfer from Ir(ppy)$_3$ to the $TolSQ-Sc^{3+}$ complex in Figure 6 by taking into account the difference in the E_{ox} values between $AcrD_2$ (0.81 V)[21] and Ir(ppy)$_3$ (0.71 V). If the difference in the free energy change of electron transfer is directly reflected in the k_{et} value, the k_{et} value of $AcrD_2$ would be smaller than that of Ir(ppy)$_3$ by $\exp(0.10F/RT)$ in which F is the Faraday constant, R is the gas constant, and $T = 298$ K. The $\exp(0.10F/RT)$ value is obtained as 48. Figure 8 shows the estimated dependence of k_{et} of Sc^{3+}-promoted electron transfer from $AcrD_2$ to the $TolSQ-Sc^{3+}$ complex (dashed line), which is simply obtained by dividing the k_{et} value of Sc^{3+}-promoted electron transfer from Ir(ppy)$_3$ to the $TolSQ-Sc^{3+}$ complex by 48. The slope of the observed linear correlation between k_D and [Sc^{3+}], $(9.5 \pm 0.1) \times 10^2$ M^{-2} s^{-1}, agrees well with that expected from the electron-transfer reaction, $(9.3 \pm 0.1) \times 10^2$ M^{-2} s^{-1}. Such agreement strongly indicates that the hydride transfer from $AcrD_2$ to the $TolSQ-Sc^{3+}$ complex proceeds via the Sc^{3+}-

(65) It should be noted, however, uncertainty of the determination of E_{red} value in the presence of Sc^{3+} (±0.05 V) due to the instability of the Sc^{3+} complexes of $TolSQ^{\bullet-}$ results in a relatively large error (±0.8) in terms of log K_1 value.

Scheme 6. Hydride-Transfer Mechanism at 298 K

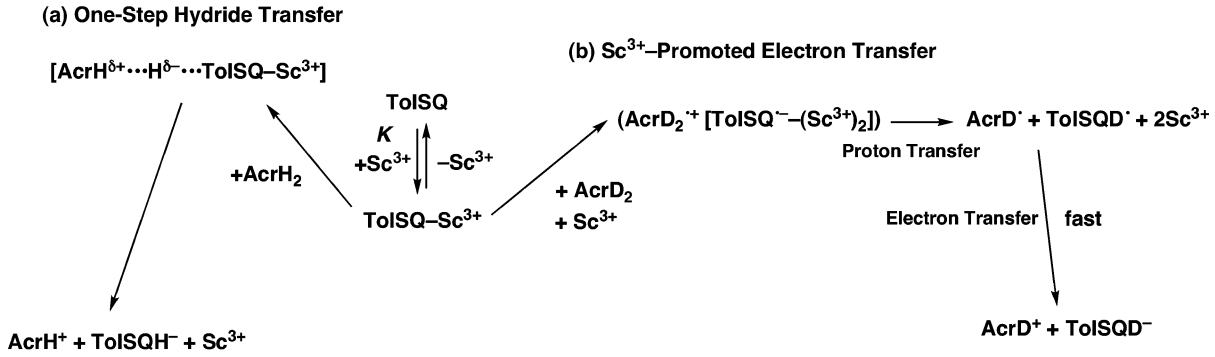

promoted electron-transfer pathway (Scheme 6b) rather than the one-step hydride-transfer pathway (Scheme 6a).

The free energy change of electron transfer from $AcrD_2$ to TolSQ is highly positive judging from the E_{ox} value of $AcrD_2$ (E_{ox} vs SCE = 0.81 V)[21] and the E_{red} value of TolSQ (E_{red} vs SCE = −0.26 V), and electron transfer from $AcrD_2$ to TolSQ is thermodynamically unlikely to occur. In the presence of Sc^{3+}, however, the E_{red} value is significantly shifted according to eq 5 (vide supra). Although the free energy change of electron transfer is still slightly positive, electron transfer is followed by proton transfer from $AcrD_2^{\bullet+}$ to the Sc^{3+} complexes of $TolSQ^{\bullet-}$. If proton transfer from $AcrD_2^{\bullet+}$ to $TolSQ^{\bullet-}$ is much faster than the initial electron transfer from $AcrH_2$ to TolSQ, the rate-determining step would be the electron transfer when there should be no kinetic isotope effect. In the presence of Sc^{3+}, however, the basicity of $TolSQ^{\bullet-}$ is reduced significantly by the complex formation with Sc^{3+} [$TolSQ^{\bullet-}$–Sc^{3+} and $TolSQ^{\bullet-}$–$(Sc^{3+})_2$]. In such a case, proton transfer from $AcrD_2^{\bullet+}$ to the $TolSQ^{\bullet-}$–Sc^{3+} and $TolSQ^{\bullet-}$–$(Sc^{3+})_2$ complexes may be slow enough to be involved in the rate-determining step. Thus, the observation of a kinetic isotope effect ($k_H/k_D = 2.5 \pm 0.3$) indicates that the proton-transfer step is at least partially involved in the rate-determining step when the electron-transfer step is coupled with the proton-transfer step. The subsequent electron transfer from $AcrD^{\bullet}$ to $TolSQD^{\bullet}$ may be highly exergonic because of the low oxidation potential of $AcrD^{\bullet}$ ($E_{ox} = -0.43$ V)[23] to yield $AcrD^+$ and $TolSQD^-$ (Scheme 6b). Thus, the overall hydride-transfer reaction may also be highly exergonic.

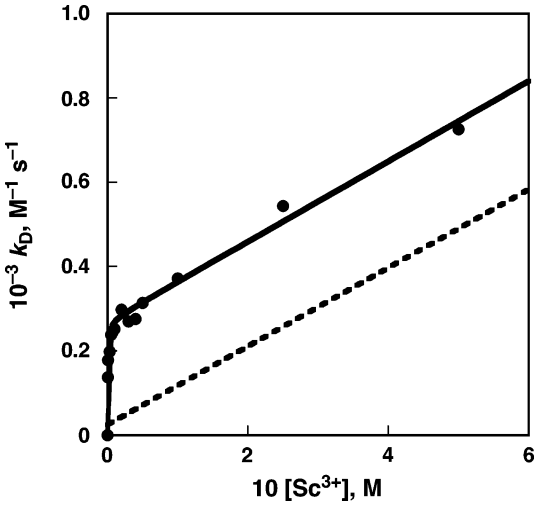

Figure 8. Dependence of k_D (●) on [Sc^{3+}] for hydride transfer from $AcrD_2$ (3.0×10^{-5} M) to TolSQ in the presence of Sc^{3+} in deaerated MeCN at 298 K. The dashed line shows the second-order rate constants of electron transfer from $AcrD_2$ to TolSQ in the presence of Sc^{3+} expected from the dependence of the second-order rate constant (k_{et}) on [Sc^{3+}] for electron transfer from $Ir(ppy)_3$ to TolSQ in the presence of Sc^{3+}.

Table 1. Activation Energies (E_a) of Hydride Transfer from $AcrH_2$ and $AcrD_2$ to TolSQ in the Presence of Sc^{3+} (1.0×10^{-2} M and 2.5×10^{-1} M) in Deaerated MeCN

	E_a[a] (kcal mol^{-1})	
NADH analogue	1.0×10^{-2} M[b]	2.5×10^{-1} M[b]
$AcrH_2$	9.9 ± 0.2	4.3 ± 0.3[c] (9.8 ± 0.2)[d]
$AcrD_2$	9.4 ± 0.2	4.6 ± 0.3

[a] Determined by the Arrhenius plots of the rate constants of the hydride-transfer reactions. [b] Concentration of Sc^{3+}. [c] Determined from the linear plot of ln k_H vs T^{-1} in the temperature range 233−283 K. [d] Determined from the linear plot of ln k_H vs T^{-1} in the temperature range 298−333 K.

The mechanistic changeover from the one-step hydride-transfer to the electron-transfer pathway by the deuterium substitution of $AcrH_2$ by $AcrD_2$ (Figure 3a) may result from a significant primary kinetic deuterium isotope effect in the direct one-step hydride transfer from $AcrD_2$ to the TolSQ–Sc^{3+} complex, when the rate constant of direct one-step hydride transfer from $AcrD_2$ becomes much smaller than that of the Sc^{3+}-promoted electron transfer from $AcrD_2$ to the TolSQ–Sc^{3+} complex.

Mechanistic Changeover by Simple Changes of Temperature and Sc^{3+} Concentration. An Arrhenius plot for the Sc^{3+}-promoted hydride transfer from $AcrH_2$ to the TolSQ–Sc^{3+} complex in the presence of a high concentration of Sc^{3+} (2.5×10^{-1} M) in Figure 4a (red open circles) showed two distinct regions (233−298 K and 298−333 K) with different slopes, indicating the occurrence of the mechanistic changeover. The break in the Arrhenius plot corresponds to a temperature (298 K) to be related to the borderline between the one-step hydride-transfer and electron-transfer pathways. The activation energies (E_a) derived from the slopes of Arrhenius plots for the Sc^{3+}-promoted hydride transfer from $AcrH_2$ and $AcrD_2$ to the TolSQ–Sc^{3+} complex in the presence of a low concentration of Sc^{3+} (1.0×10^{-2} M) and a high concentration of Sc^{3+} (2.5×10^{-1} M) are summarized in Table 1. There are two types of E_a values: one is 9.6 ± 0.5 kcal mol^{-1} for the Sc^{3+}-promoted hydride transfer from $AcrH_2$ and $AcrD_2$ to the TolSQ–Sc^{3+} complex in the presence of a low concentration of Sc^{3+} (1.0×10^{-2} M), and the other is 4.5 ± 0.5 kcal mol^{-1} for the Sc^{3+}-promoted hydride transfer from $AcrH_2$ and $AcrD_2$ to the TolSQ–Sc^{3+} complex in the presence of a high concentration of Sc^{3+} (2.5×10^{-1} M). The higher E_a value (9.6 ± 0.5 kcal mol^{-1}) corresponds to that of the one-step hydride-transfer pathway, and the smaller E_a value (4.5 ± 0.5 kcal mol^{-1})

corresponds to that of the electron-transfer pathway. In the case of the Sc^{3+}-promoted hydride transfer from $AcrH_2$ to the TolSQ−Sc^{3+} complex in the presence of a high concentration of Sc^{3+} (2.5×10^{-1} M), the changeover of the pathways occurs at 298 K from the electron transfer (233−298 K) with $E_a = 4.5 \pm 0.5$ kcal mol^{-1} to the one-step hydride transfer (298−333 K) with $E_a = 9.6 \pm 0.5$ kcal mol^{-1}. The changeover of the reaction pathways results from the E_a and A (pre-exponential factor) values of the one-step hydride-transfer pathway being larger than those of the electron-transfer pathway. The smaller E_a value of the electron-transfer pathway is ascribed to the strong binding of Sc^{3+} ions in the 1:2 complex of $TolSQ^{\bullet-}$ with Sc^{3+} [$TolSQ^{\bullet-}$−$(Sc^{3+})_2$], which results in stabilization of the transition state as well as the electron-transfer product.

The smaller A value of the electron-transfer pathway may also result from the formation of $TolSQ^{\bullet-}$−$(Sc^{3+})_2$ where a higher degree of organization of Sc^{3+} ions is required as compared with that the 1:1 TolSQ−Sc^{3+} complex involved in the one-step hydride-transfer pathway.

With regard to the kinetic deuterium isotope effect (k_H/k_D), the k_H/k_D value of the one-step hydride-transfer pathway is nearly temperature independent ($k_H/k_D = 4.5 \pm 0.5$), because the E_a values of $AcrH_2$ and $AcrD_2$ are virtually the same (Table 1). Such a temperature independent kinetic deuterium isotope effect suggests that the transition state of the one-step hydride-transfer pathway is nonlinear when the amplitudes of H vibration are considerably less restricted in a bent transition state as discussed by Kwart.[66] In contrast with the large k_H/k_D value for the one-step hydride-transfer pathway, the k_H/k_D value of the electron-transfer pathway, followed by proton transfer ($k_H/k_D = 2.5 \pm 0.3$), is significantly smaller, but the observation of the kinetic deuterium isotope effect in the electron-transfer pathway indicates that the proton transfer from $AcrH_2^{\bullet+}$ to $TolSQ^{\bullet-}$−$(Sc^{3+})_2$ following the Sc^{3+}-promoted electron transfer is also involved in the rate-determining step (vide supra).

Summary and Conclusions

Hydride transfer from an NADH analogue, 9,10-dihydro-10-methylacridine ($AcrH_2$) to 1-(*p*-tolylsulfinyl)-2,5-benzoquinone (TolSQ) occurs efficiently in the presence of Sc^{3+}, whereas no hydride-transfer reaction occurs in the absence of Sc^{3+}. The hydride-transfer reaction of $AcrH_2$ occurs via direct one-step hydride transfer from $AcrH_2$ to the TolSQ−Sc^{3+} complex formed between TolSQ and Sc^{3+} at 298 K. In such a case, the k_H value increases exhibiting a saturated behavior with respect to Sc^{3+} concentration ([Sc^{3+}]), when almost all TolSQ molecules form the TolSQ−Sc^{3+} complex. The one-step hydride-transfer mechanism is changed to electron transfer followed by proton and electron transfer by deuterium substitution of $AcrH_2$ by $AcrD_2$. The k_D value increases linearly with an increase in [Sc^{3+}]. Similarly, the rate constant of electron transfer (k_{et}) from the electron donor tris(2-phenylpyridine)iridium [$Ir(ppy)_3$] to TolSQ increases linearly with increasing [Sc^{3+}]. Such a first-order dependence of k_H and k_{et} on [Sc^{3+}] is ascribed to formation of a 1:2 complex between $TolSQ^{\bullet-}$ and Sc^{3+} [$TolSQ^{\bullet-}$−$(Sc^{3+})_2$], which was detected by ESR. The one-step hydride-transfer pathway is also changed to the electron-transfer pathway with decreasing temperature due to the larger E_a and A values of the one-step hydride-transfer pathway than those of the electron-transfer pathway. A break is observed in the Arrhenius plot for the Sc^{3+}-promoted hydride-transfer reaction of $AcrH_2$, corresponding to the borderline between the one-step hydride-transfer and electron-transfer pathways.

Acknowledgment. This work was partially supported by Grants-in-Aid (No. 16205020) from the Ministry of Education, Culture, Sports, Science and Technology, Japan.

Supporting Information Available: First-order plots for hydride transfer from $AcrH_2$ to TolSQ in the presence of Sc^{3+} (S1), dependence of k_{obs} on [TolSQ] (S2), cyclic voltammograms of TolSQ and $Ir(ppy)_3$ (S3), cyclic voltammogram of TolSQ in the presence of Sc^{3+} (S4), first-order plot for Sc^{3+}-promoted electron transfer from $Ir(ppy)_3$ to TolSQ (S5), dependence of k_{obs} on [TolSQ] (S6), plot of k_H^{-1} vs $[Sc^{3+}]^{-1}$ (S7), absorption spectra of TolSQ in the presence of various concentrations of Sc^{3+} (S8), plot of $k_{et}(1 + K[Sc^{3+}])/(K[Sc^{3+}])$ vs [Sc^{3+}] (S9). This material is available free of charge via the Internet at http://pubs.acs.org.

JA064708A

(66) Kwart, H. *Acc. Chem. Res.* **1982**, *15*, 401.